The Analyst COMMUNICATION

Single-molecule detection using confocal fluorescence detection: Assessment of optical probe volumes

Elisabeth K. Hill and Andrew J. de Mello*

Zeneca/SmithKline Beecham Centre for Analytical Science, Department of Chemistry, Imperial College of Science, Technology and Medicine, London, UK SW7 2AY. E-mail: a.demello@ic.ac.uk

Received 20th March 2000, Accepted 11th April 2000
Published on the Web 4th May 2000

We have constructed a simple component-based confocal detection system, that is capable of fluorescence detection at the single-molecule level. The component-based format maximises flexibility and reduces start-up costs. A new model for the optical probe volume is proposed, that is based on the $1/e^2$ Gaussian intensity contour of a laser beam focused to the diffraction limit. Observation of the onset of single-molecule detection in our experimental system confirms that this model is more appropriate than a simple cylindrical approximation for a probe volume defined by a wide, tightly focused laser beam.

Introduction

In the last decade, techniques have been developed that demonstrate ultrasensitive fluorescence detection at the individual molecular level. Single-molecule detection (SMD) in solution has been reported for several classes of fluorophore and applied to several regimes. Ambrose *et al.* have recently provided a comprehensive overview of the field.[1]

Miniaturisation of conventional laboratory instrumentation has also been the focus of much attention in recent years.[2] Advantages of 'downsizing' analytical processes lie in improved efficiency with respect to throughput, cost, response time, sample volumes and automation. Indeed, microfabricated instruments, commonly termed miniaturised total analysis systems (μ-TAS), have been successfully applied to many areas of chemical analysis, including separation science, DNA analysis, DNA amplification, immunoassays, small molecule synthesis and cell manipulation.[3] Adaptation of conventional detection methods to measurement in small volumes has closely accompanied the development of μ-TAS, and will ultimately determine true system utility. Consequently, the development and application of SMD to μ-TAS is currently of considerable interest.

One method to achieve single-molecule detection sensitivity adopts the principle of confocal detection[4,5] (Fig. 1a). A pinhole positioned in the confocal plane of a microscope objective rejects all light except that which originates from the focal point.[6,7] The volume interrogated is restricted to the region illuminated by the laser beam in the vicinity of the focal point (typically a few femtolitres, 10^{-15} L). When a dilute solution ($\sim 10^{-9}$ M) is examined, there is on average one fluorescent molecule or less resident in the probe volume. Use of a high numerical aperture immersion objective maximises the fluorescence collection efficiency, and a dichroic beamsplitter discriminates between excitation and emission wavelengths. A single objective for both illumination and fluorescence collection guarantees superposition of excitation and detection optics in the focal region. Motion of the analyte molecules through the detection volume is usually diffusion mediated, although other flow-based systems are possible.[8,9]

The inherent versatility of confocal detection makes it our method of choice for ultrasensitive fluorescence studies. The system is flexible and offers us the possibility of modification and adaptation for a range of sample formats, subject to the working distance constraint of a high numerical aperture microscope objective (~ 170 μm). Therefore diversification to chip based assays should pose no further optical detection challenges.

Commercial confocal microscopy systems can be prohibitively costly, and modification of a standard microscope may be complex. In this communication we report an inexpensive and adaptable confocal fluorescence excitation and detection system that is built from simple optical components. We have used the system to directly observe the onset of a single-molecule detection (SMD) regime in serial dilutions of selected fluorophores and record individual fluorescence bursts in real time with continuous wave (CW) excitation. We also present a model of optical probe volumes in the Gaussian limit and demonstrate that, for our experimental conditions, a simple cylindrical approximation for the beam waist may grossly underestimate the probe volume.

Experimental methods

Apparatus

The main optical elements of a confocal microscope are retained in the experimental setup as illustrated in Fig. 1b. The excitation source is a CW air-cooled argon ion laser operated in light control mode at 488 nm and 7.0 mW (Omnichrome; Melles Griot, Cambridge, UK). The use of light at 488 nm complements conventional protocols in fluorescence microscopy: an extensive catalogue of fluorescent dyes has been

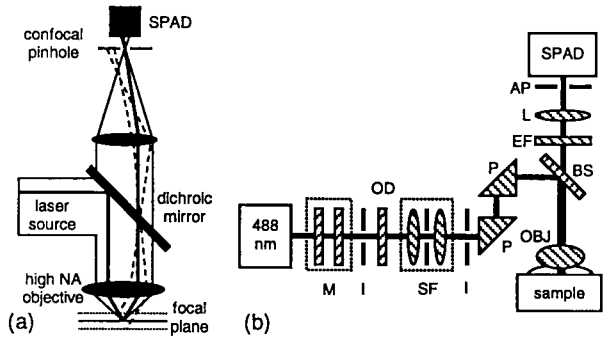

Fig. 1 (a) Principle of confocal detection. A confocal pinhole only selects light that emanates from the focal region. Dashed lines indicate paths of light sampled above and below the focal plane that are rejected at the pinhole. (b) Schematic diagram of the component-based confocal detection optics. (M, mirror; I, adjustable iris; OD, neutral density filter; SF, spatial filter; P, right-angled prism; OBJ, 100× microscope objective; BS, dichroic beamsplitter; EF, emission filter; L, lens; AP, confocal aperture.

developed for this excitation wavelength.[10] Beamsteering optics (mirrors, prisms, irises) direct the light into the confocal system. Glass neutral density filters attenuate the laser intensity as required (OD 0.2–3.0; Newport Ltd., Newbury, UK). The laser beam is spatially filtered (5-axis compact filter; Newport Ltd.) in order to ensure a near-Gaussian intensity profile.

The dichroic mirror (505DRLP02; Omega Optical, Brattleboro, VT, US) is oriented at 45° to reflect 488 nm radiation and so define a vertical axis, normal to the surface of the optical table. This alignment is checked with a small mirror in the sample position; superposition of the incident and reflected beams along the entire optical path guarantees normal incidence. An infinity corrected, high numerical aperture (NA) microscope objective brings the light to a tight focus (Fluar 100×/1.3 NA, oil immersion; Carl Zeiss Ltd., Welwyn Garden City, UK). The collimated laser beam has a $1/e^2$ diameter of 2.5 mm. This width is selected to nearly fill the back of the microscope objective, and so attain a beam focus estimated to be close to the diffraction limit.

Samples were contained in a microscope slide with a small well and imaged beneath a thin glass cover slip (grade 0; BDH Merck, Poole, Dorset, UK) with a drop of immersion oil (Immersol, n = 1.518; Carl Zeiss Ltd.). The sample volume was typically 270 μL.

Fluorescence emitted by the sample is collected by the same high NA objective and transmitted through the dichroic mirror. An emission filter (515EFLP; Omega Optical) removes any residual excitation light. A plano-convex lens (+50.2F; Newport Ltd.) focuses the fluorescence onto a precision pinhole (25 or 50 μm; Melles Griot) placed immediately in front of the detector. The pinhole is positioned in the confocal plane of the microscope objective. All lenses and prisms are coated with a dielectric broadband anti-reflection coating to reduce reflection losses.

The detector is a silicon avalanche photodiode operating in single-photon counting mode (SPCM-AQ-131; EG&G Canada, Vaudreuil, Quebec, Canada). The avalanche photodiode is selected for its high quantum efficiency ($P_{d,max}$ = 70%) and acceptably low dark count rate (< 160 Hz). The electronic signal from the detector is coupled to a data acquisition card operating in multichannel scaler mode. (PCA-3; Oxford Instruments, Oxford, UK, running on 100 MHz Pentium PC). Alignment of the pinhole and detector was optimised before each measurement.

Materials

R-Phycoerythrin solution was purchased from Molecular Probes (Eugene, OR, USA) and stored in the dark below 4 °C; Rhodamine 6G chloride was from Exciton (Dayton, OH, USA). 18 MΩcm^{-1} grade UHQ water was from a Milli-Q50 system (Millipore, Watford, UK). All solvents and buffer solutions were spectroscopic grade from BDH Merck or Sigma-Aldrich/Fluka (Poole, Dorset, UK) and were used as received. Solutions were prepared by serial dilution from 10 μM primary and 100 nM secondary stock solutions. Glassware was cleaned in Decon '90 solution (Fisher Scientific, Loughborough Leics., UK) and rinsed several times in UHQ water before use.

Theory

Modelling the confocal probe volume

In much of the literature to date, the confocal probe volume is approximated as a cylinder with a radius defined by the diffraction limited waist of a Gaussian beam.[4,11] An alternative model would consider the Gaussian profile of the focused beam. Here we present such a model, and compare the probe volumes predicted in each approach.

The $1/e^2$ intensity contour radius of a Gaussian waveform with wavelength, λ, at some distance, z, from the beam waist radius, w_o, is given by eqn. (1).[12]

$$w(z) = w_o\sqrt{1+\left(\frac{\lambda_z}{\pi w_o^2}\right)^2} \quad (1)$$

We define our system as shown in Fig. 2a, then the probe volume, V, is given by the volume of rotation of $w(z)$ around the z-axis between Z' and $-Z'$.

$$V = \int_{-z'}^{z'} \pi w(z)^2 \,dz = \int_{-z'}^{z'} w_o^2\left(1+\left(\frac{\lambda z}{\pi w_o^2}\right)^2\right)dz$$

$$V = \pi\left[w_o^2 z + w_o^2\left(\frac{\lambda}{\pi w_o^2}\right)^2\frac{z^3}{3}\right]_{-z'}^{z'} = 2\pi w_o^2 Z' + \frac{2\lambda^2}{3\pi w_o^2}Z'^3 \quad (2)$$

The Gaussian volume expression contains two terms. The first term, $2\pi w_o^2 Z'$, corresponds to the central cylindrical volume; the second term has a more complex form that describes the extra curved volume (Fig. 2b). Gaussian theory[4] also gives the diffraction-limited beam waist radius, w_o, in terms of the focusing objective focal length, f, and the collimated beam radius, R.

$$w_o = \frac{\lambda f}{n\pi R} \quad (3)$$

n is the refractive index.

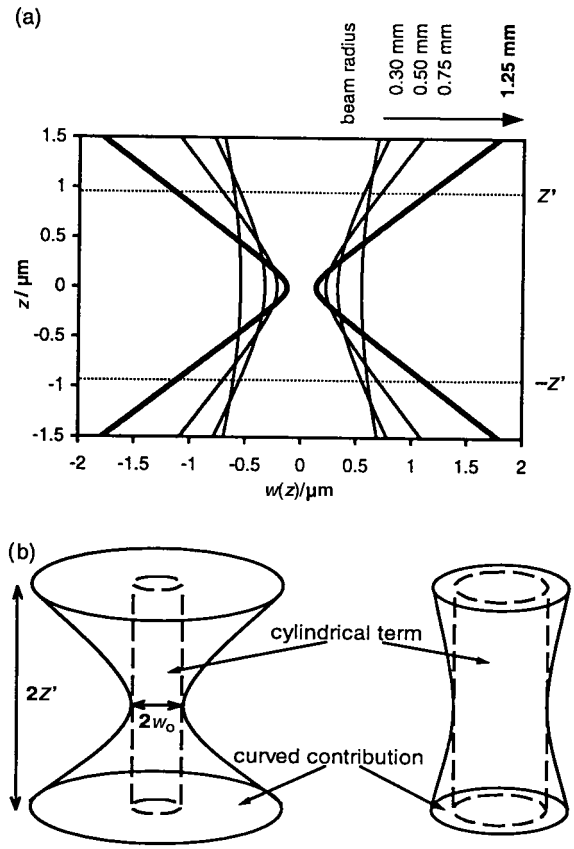

Fig. 2 (a) $1/e^2$ Gaussian intensity contours (eqn. (1)) plotted for a series of laser beam radii. λ = 488 nm, f = 1.6 mm, n = 1.52; (b) Cylindrical and curved components of the Gaussian probe volume. The curved contribution is more significant for large beam diameters and correspondingly tight beam waists.

Substitution in eqn. (2) gives:

$$V = 2\pi\left(\frac{\lambda f}{n\pi R}\right)^2 Z' + \frac{2\lambda^2}{3\pi}\left(\frac{n\pi R}{\lambda f}\right)^2 Z'^3 = \frac{2\lambda^2 f^2}{\pi n^2 R^2} Z' + \frac{2\pi n^2 R^2}{3 f^2} Z'^3 \quad (4)$$

The volume is now expressed in terms of identifiable experimental variables and constants. (Probe depth, Z', is limited by the aperture diameter.) Once again, the first term may be correlated with the cylindrical contribution to the volume, and the second term is the extra volume due to the curved contour. Fig. 2a shows the nature of the dependence of the diffraction limited waist on the collimated beam radius. It is clear that, for a given focal length, the non-cylindrical contribution to the probe volume will increase with beam diameter, when the diffraction limited focus is correspondingly sharp and narrow. This is the case in our experimental system: a broad laser beam (diameter *ca.* 2.5 mm) is employed to nearly backfill the microscope objective and ensure a focus that is close to the diffraction limit.

The two models are similar for narrow beam widths or shallow probe depths. These conditions generate probe volumes most like a cylinder. Variations occur in systems where the laser beam is broad. For example, given λ = 488 nm, f = 1.6 mm, n = 1.52 and Z' = 0.5 μm, the diffraction-limited focus of a 2.5 mm beam defines a volume that is 0.05 fL in the cylindrical approximation, and 0.42 fL in the Gaussian model, whereas the values for a 1.0 mm beam are 0.33 fL and 0.40 fL, respectively.

The assumptions in this Gaussian model are that the laser beam has a true Gaussian form, and that the beam focus is diffraction limited. Aberrations in the objective lens are assumed to be smaller than the diffraction limit. This is likely for a highly corrected optic. It is also important to note that the detection probe volume will have a strongly non-uniform intensity distribution. The fluorescence intensities, observed as photon burst sizes, will be dependent on the laser intensity experienced, and therefore on the location of the molecule within the beam.

In principle, the probe depth or depth of focus is determined by the convolution of the point spread function and collection efficiency function.[7] We estimate the axial resolution ($2Z'$) to be 1 μm.

Results and discussion

Fig. 3a and b show some indicative results from the system. The scans show fluorescence bursts for a 1 nM solution of R-phycoerythrin (R-PE) in a pH 7 phosphate buffer, and for 300 pM Rhodamine 6G (R6G) in glycerol. Fluorescence photon bursts due to single-molecule events are clearly distinguished above a low background baseline of less than 8 counts per channel in the raw data (R-PE/buffer). It is noticeable that the bursts vary in height and size. This is due in part to the range of possible molecular trajectories through the probe volume and to photobleaching kinetics, but it is also an indirect indication of a strongly non-uniform illumination intensity in the probe region. Near the beam waist the laser intensity is greatest, and it drops off rapidly towards the edges and ends of the probe volume. The fluorescence emission intensity will follow this variation.

Observation of the fluctuation in fluorescence collected from progressively more dilute samples enables us to examine the onset of a single-molecule detection regime. We observe clearly separated bursts in solutions less than 2 nM in fluorescent analyte, although scans in 5 nM solutions show more unstructured fluctuation. This is consistent with probe volume occupation probabilities calculated according to a Poisson distribution; values for sparse-molecule and single-molecule regimes are listed in Table 1.

For 2 nM solutions the probability for two or more fluorescent molecules to be simultaneously resident in the optical probe volume is less than 10%. This probability drops beneath

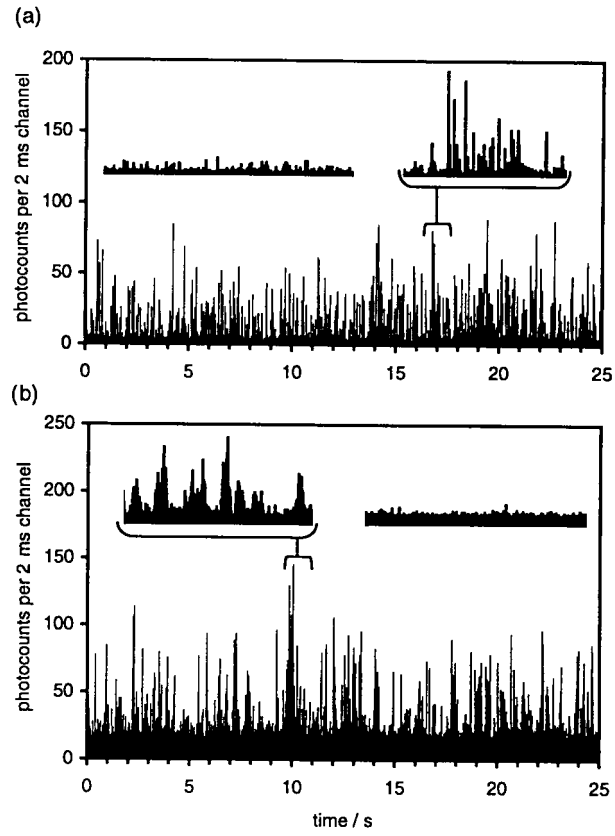

Fig. 3 Representative single-molecule fluorescence bursts. (a) 1 nM R-phycoerythrin in pH 7 phosphate buffer, laser power approximately 10 μW. (b) ~300 pM acidified Rhodamine 6G in glycerol, laser intensity approximately 50 μW. Insets show background levels and expanded burst details. Acquisition time: 2 ms per data point.

Table 1 Instantaneous occupation probabilities above and below the single-molecule limit calculated for an optical probe volume of 0.42 fL. An underlying Poisson distribution is assumed, with distribution parameter k, equal to the mean number of molecules per probe volume (Blank entries in the table are probabilities < 0.1%)

Bulk analyte concentrations	Mean number density (k)/molecules per probe volume	Instantaneous occupation probability calculated according to Poisson statistics, $P(x) = e^{-k}k^x/x!$[a]							
		$P(0)$	$P(1)$	$P(2)$	$P(3)$	$P(4)$	$P(5)$	$P(10)$	$P(0,1)$
10 nM	2.55	0.078	0.200	0.254	0.216	0.137	0.070	0.002	0.278
5 nM	1.27	0.280	0.356	0.227	0.096	0.031	0.008	—	0.636
2 nM	0.51	0.601	0.306	0.078	0.013	0.002	—	—	0.907
1 nM	0.25	0.775	0.197	0.025	0.002	—	—	—	0.973
500 pM	0.13	0.880	0.112	0.007	—	—	—	—	0.993
300 pM	0.08	0.926	0.071	0.003	—	—	—	—	0.997

[a] Where k is the mean and variance of the distribution.

2.5% for 1nM solutions and below. These multiple occupancies will include transient events; *i.e.*, the overlap occurs for a fraction of the residence time. In a cylindrical model with diameter approximately $2w_o$ = 260 nm and a volume of 0.05 fL, single-molecule detection should be possible in a 30 nM solution. However, the onset of SMD observed between 5 nM and 2 nM supports the Gaussian model for our probe volume of 0.42 fL.

Autocorrelation values were calculated for the experimental data, and fitted to the standard autocorrelation function for a particle diffusing through a Gaussian beam.[13] Values of the diffusion coefficients so obtained are in accord with reported literature values, and the fitted spatial parameters also support the magnitude of the probe volume. We obtain diffusion values of 10^{-11} m^2 s^{-1} for R-PE, using a non-linear least squares minimisation routine to fit a series of autocorrelation curves. The diffusion coefficient of aqueous phycoerythrin has been reported elsewhere[14] as 4×10^{-11} m^2 s^{-1}.

Modification of the viscosity of the solvent will result in modification of the diffusion coefficient of the system. This will manifest itself in altered probe volume residence times and fluorescence burst widths, providing the molecule is not photobleached. Rhodamine 6G in glycerol exhibits longer burst widths (Fig. 3b), and autocorrelation analysis supports a smaller diffusion coefficient. R-PE in aqueous sucrose solutions of escalating concentration (increasing viscosity) also demonstrate reduced diffusion coefficients (increased diffusion times) and lengthened fluorescence bursts.

The component-based confocal fluorescence detection system we have constructed is simple, inexpensive, yet demonstrably capable of ultrasensitive detection down to single-molecule limits. We have attained single-molecule detection limits for an individual fluorophore (R6G), and in a biologically relevant system (R-PE). We have also observed single-molecule fluorescence in other dye systems. The in-built flexibility of the system will facilitate application to miniaturised sample formats, *e.g.*, microchip-based assays. Work is in progress to achieve single-molecule fluorescence detection in biologically relevant systems on μ-TAS devices.

Acknowledgement

E. H. is grateful to SmithKline Beecham Pharmaceuticals for an EPSRC CASE studentship.

References

1 W. P. Ambrose, P. M. Goodwin, J. H. Jett, A. van Orden, J. H. Werner and R. A. Keller, *Chem. Rev.*, 1999, **99**, 2929.
2 M. U. Kopp, H. J. Crabtree and A. Manz, *Curr. Opin. Chem. Biol.*, 1997, **1**, 410.
3 S. C. Jakeway, A. J. de Mello and E. Russell, *Fresenius' J. Anal. Chem.*, 2000, **366**, 525.
4 S. M. Nie, D. T. Chiu and R. N. Zare, *Anal. Chem.*, 1995, **67**, 2849.
5 M. A. Osborne, S. Balasubramanian, W. S. Furey and D. Klenerman, *J. Phys. Chem. B*, 1998, **102**, 3160.
6 *Handbook of Biological Confocal Microscopy*, ed. J. B. Pawley, Plenum Press, London, 2nd edn., 1995.
7 R. H. Webb, *Rep. Prog. Phys.*, 1996, **59**, 427.
8 W. A. Lyon and S. M. Nie, *Anal. Chem.*, 1997, **69**, 3400.
9 C. Zander, K. H. Drexhage, K. T. Han, J. Wolfrum and M. Sauer, *Chem. Phys. Lett.*, 1998, **286**, 457.
10 *Handbook of Fluorescent Probes and Research Chemicals*, ed. R. P. Haugland, Molbes Inc., Oregon, 6th edn., 1996.
11 S. Nie and R. N. Zare, *Ann. Rev. Biophys. Biomol. Struct.*, 1997, **26**, 567.
12 R. D. Guenther, *Modern Optics*, Wiley, New York, 1990.
13 R. Rigler, Ü. Mets, J. Widengren and P. Kask, *Eur. Biophys. J.*, 1993, **22**, 169.
14 D. de Beer, P. Stoodley and Z. Lewandowski, *Biotechnol. Bioeng.*, 1997, **53**, 151.